Characteristics of early versus late in-stent restenosis in second-generation drug-eluting stents: an optical coherence tomography study

Lei Song[1,2,3], MD; Gary S. Mintz[1], MD; Dong Yin[1,2,3], MD; Myong Hwa Yamamoto[1,2], MD; Chee Yang Chin[1,4], MD, MSc; Mitsuaki Matsumura[1], BS; Ajay J. Kirtane[1,2], MD, SM; Manish A. Parikh[1,2], MD; Jeffrey W. Moses[1,2], MD; Ziad A. Ali[1,2], MD, DPhil; Richard A. Shlofmitz[5], MD; Akiko Maehara[1,2]*, MD

1. Cardiovascular Research Foundation, New York, NY, USA; 2. NewYork-Presbyterian Hospital/Columbia University Medical Center, New York, NY, USA; 3. National Center for Cardiovascular Disease, China Peking Union Medical College, Fuwai Hospital, Beijing, China; 4. National Heart Centre Singapore, Singapore; 5. St. Francis Hospital, Roslyn, NY, USA

KEYWORDS

- clinical research
- in-stent restenosis
- optical coherence tomography

Abstract

Aims: In-stent restenosis (ISR) is an important cause of drug-eluting stent (DES) failure and target vessel revascularisation. In this study we aimed to evaluate differences between early and late-presenting restenosis in second-generation DES using optical coherence tomography (OCT).

Methods and results: Overall, 171 cases of second-generation DES ISR with a follow-up OCT minimum lumen area <3.0 mm² were included: 33.3% of patients (n=57) had early ISR, and 66.7% (n=114) had late ISR (duration from stent implantation >1 year). Minimum stent area (MSA) <4.0 mm², neointimal thickness <100 μm, and heterogeneous neointimal hyperplasia (NIH) were more prevalent in early ISR, whereas NIH with neoatherosclerosis trended towards being more frequent for late ISR (28.9% vs. 15.8%, p=0.06). Multivariable analysis revealed that duration from implantation >2 years, absence of statin use, and NIH >50% were independent predictors for neoatherosclerosis (all p<0.05).

Conclusions: OCT morphological characteristics of second-generation DES ISR differ between early and late presentation. Early ISR was associated with MSA <4.0 mm², while neoatherosclerosis contributed more commonly to late ISR.

Corresponding author: Cardiovascular Research Foundation, 1700 Broadway, 9th Floor, New York, NY 10019, USA. E-mail: amaehara@crf.org

Abbreviations

BMS   bare metal stent
CSA   cross-sectional areas
DES   drug-eluting stent(s)
EES   everolimus-eluting stent(s)
ISR   in-stent restenosis
IVUS   intravascular ultrasound
MLA   minimum lumen area
MSA   minimum stent cross-sectional area
NIH   neointimal hyperplasia
OCT   optical coherence tomography

Introduction

Second-generation drug-eluting stents (DES) significantly reduce in-stent restenosis (ISR) and the need for repeat revascularisation compared with bare metal stents (BMS) or first-generation DES[1,2]. Furthermore, clinical evidence is consistent with less "late catch-up" in second-generation DES[3,4]; however, reintervention is still needed in approximately 5-10%, depending on the cohort, duration, and stent type[5]. Most intravascular imaging reports are based on data from first-generation DES[6,7]. The aim of this study was to use optical coherence tomography (OCT) to evaluate early and late ISR in second-generation DES.

Methods

PATIENTS

We retrospectively reviewed 483 patients (505 previously stented lesions) who underwent OCT follow-up at two sites in the United States of America (NewYork-Presbyterian Hospital, New York, NY, USA; St. Francis Hospital, Roslyn, NY, USA) from February 2011 to January 2016. ISR was defined as an OCT in-stent minimum lumen area (MLA) <3.0 mm^2 [8,9]. We excluded 189 lesions that had an MLA $\geq$3.0 mm^2: six with stent thrombosis, but not ISR; 19 with poor image quality; 14 with multiple ISR lesions (only the most severe ISR lesion was included); three ISR in a saphenous vein graft; and 103 ISR that were either first-generation DES or BMS. Second-generation DES restenosis (171 patients; 171 lesions) included PROMUS™ (Boston Scientific, Marlborough, MA, USA) everolimus-eluting stents (EES), XIENCE® (Abbott Vascular, Santa Clara, CA, USA), and Resolute™ (Medtronic, Minneapolis, MN, USA) zotarolimus-eluting stents. Early ($\leq$1 year) vs. late (>1 year) presentation was based on duration from stent implantation. Analysis included medical and intervention history, angiographic and procedural data, and OCT parameters. The study complied with the Declaration of Helsinki. The NewYork-Presbyterian Hospital and St. Francis Hospital ethics committees approved the research protocol.

Clinical ISR presentation was divided into acute coronary syndromes (including unstable angina [no ST-segment elevation and no biomarker release, but angina at rest, new-onset angina, or a crescendo pattern of angina occurrence], ST-segment elevation myocardial infarction, or non-ST-segment elevation myocardial infarction [no ST-segment elevation, but with biomarker release]) versus non-acute coronary syndromes.

Coronary angiograms were analysed by trained interventional cardiologists at the Cardiovascular Research Foundation (New York, NY, USA) using Medis CMS software, version 7.2 (Medis medical imaging systems, Leiden, the Netherlands). Minimum lumen diameter and interpolated reference vessel diameter were used to calculate diameter stenosis ([1-minimum lumen diameter/reference vessel diameter]×100). Lesion length was measured as the distance from the proximal to the distal shoulder in the projection with the least amount of foreshortening. Angiographic restenosis was classified[10] as: (1) focal ISR (Type I, defined as ISR <10 mm in length); (2) diffuse ISR (Type II, defined as ISR >10 mm length but within the stent); (3) proliferative (Type III, defined as ISR >10 mm in length but extending beyond the stent edges); and (4) total occlusion (Type IV).

OCT IMAGING AND ANALYSIS

An OCT catheter (C7 Dragonfly™ or Dragonfly™ Duo; St. Jude Medical, St. Paul, MN, USA) was introduced distal to the lesion, and contrast media was injected via the guiding catheter at a rate of 3-4 mL/s during pullback. OCT images were acquired using frequency-domain OCT (C7-XR™, ILUMIEN™, or ILUMIEN™ OPTIS™ OCT imaging systems; St. Jude Medical) at 100 or 180 frames/s at a pullback speed of 20-25 mm/s as described[11]. Off-line analysis was carried out by agreement of two independent cardiologists (L. Song and A. Maehara) blinded to patient baseline clinical and angiographic characteristics and using proprietary software (St. Jude Medical) after confirming calibration settings.

All cross-sectional OCT slices were evaluated, and stent and intra-stent lumen cross-sectional areas (CSA) were measured for slices with the minimum lumen CSA, minimum stent CSA (MSA), and maximum neointimal hyperplasia (NIH) CSA as reported[12]. Stent CSA was measured by joining middle points of the strut blooming. If the stent was covered by high signal attenuation tissue, stent CSA was delineated using proximal and distal slices. The percentage of NIH was calculated as ([stent–lumen CSA]/stent CSA)×100. Proximal and distal reference lumen CSAs were the slices with the largest lumen CSA within 5 mm proximal and distal to the stent edges, but before significant side branches (>1.5 mm in diameter). Underexpansion was defined as MSA <4.0 mm^2.

Neoatherosclerosis was defined as NIH within the ISR segment that contained lipid, calcification, or neointimal rupture[13]. The distribution of neoatherosclerosis was categorised as: 1) focal (<10 mm in length); 2) multifocal (<10 mm in length and >5 mm apart); or 3) diffuse ($\geq$10 mm in length). Lipidic NIH was a signal-poor region with diffuse borders; a thin-cap fibroatheroma had fibrous cap thickness $\leq$65 µm within lipidic NIH **(Figure 1A)**[6,7]. Neointimal calcium was a signal-poor area with a well-delineated border with the underlying NIH **(Figure 1B)**. Neointimal rupture referred to a break in the fibrous cap connecting the lumen with the underlying lipidic NIH **(Figure 1C)**. Tissue at the MLA site within the stented segment was assessed qualitatively to characterise the pattern of neointima as neoatherosclerosis or non-neoatherosclerotic tissue (homogeneous
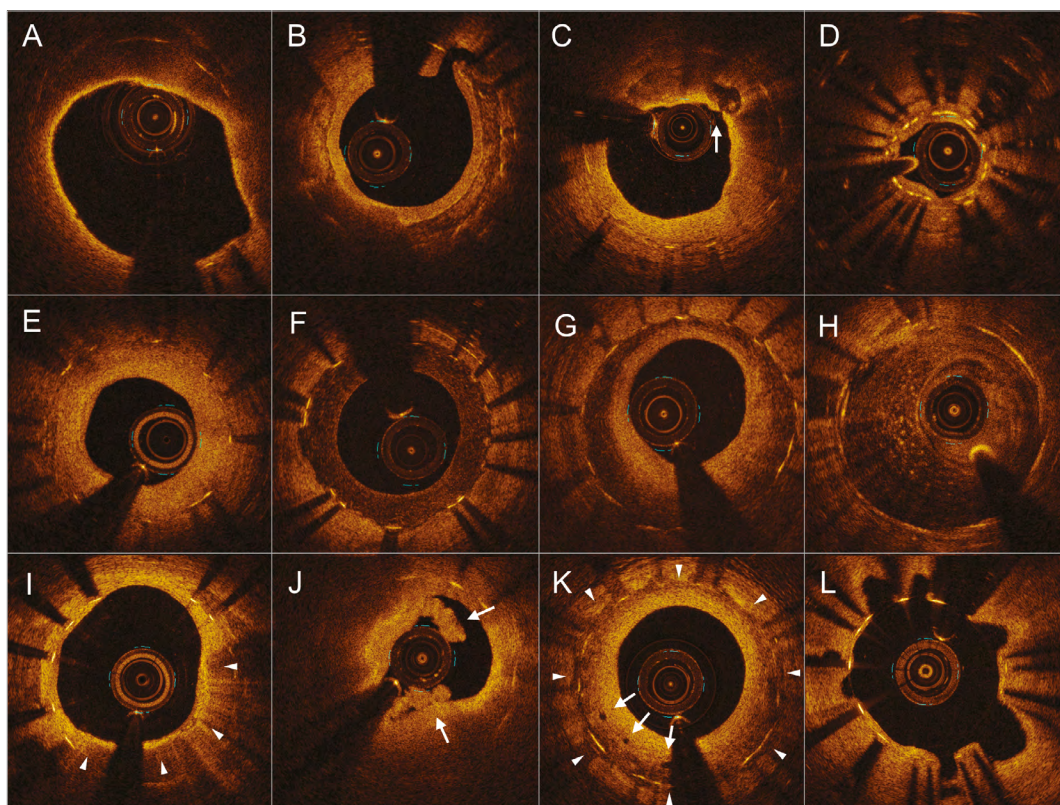
Figure 1. *Representative optical coherence tomography images of various vascular morphologies. A) Lipidic neointimal hyperplasia, thin-cap fibroatheroma. B) Neointimal calcium. C) Neointimal rupture (arrow). D) Intimal thickness <100 μm (underexpanded stent). E) Homogenous hyperplasia, high-intensity. F) Homogenous hyperplasia, low-intensity. G) Heterogeneous hyperplasia, layered pattern. H) Heterogeneous hyperplasia, non-layered pattern. I) Macrophage accumulation in neointimal hyperplasia (triangles). J) Thrombus (arrows) without rupture with lipidic neointimal hyperplasia. K) Peri-strut low-intensity area (triangles) and microvessels (arrows). L) Evagination.*

or heterogeneous tissue or mean neointimal thickness <100 μm) **(Figure 1D)**. Homogeneous restenotic tissue showed uniform signal properties (high intensity or low intensity) without focal variation or attenuation (**Figure 1E**, **Figure 1F**)[11]. Heterogeneous restenotic tissue had variable optical properties and backscattering patterns and was divided into layered vs. non-layered (**Figure 1G**, **Figure 1H**): a layered pattern of heterogeneous neointimal tissue consisted of concentric layers with an endoluminal high backscattering layer and an abluminal layer with low backscattering optical properties. Macrophage accumulation was a high-intensity, signal-rich, linear region with sharp attenuation and a narrow trailing shadow that changed frame by frame **(Figure 1I)**. Thrombus **(Figure 1J)**, microvessels, and peri-strut low-intensity areas were also noted as reported **(Figure 1K)**[6,7,12-14].

A malapposed strut was a strut with a measured distance between its surface and the adjacent vessel surface greater than the sum of the thickness of the strut plus polymer (zotarolimus-eluting stents ≥110 μm; EES ≥100 μm). Malapposition distance was measured from the centre of the strut blooming to the adjacent lumen border[12]. Coronary evagination was the presence of an outward protrusion in the luminal vessel contour between well-apposed struts with a maximum depth of the protrusion >10% of

mean stent diameter within the same frame **(Figure 1L)**[15]. Stent fracture was classified as a separation of the stent into two pieces separated by image slices with ≥120° of the stent circumference having no visible struts. Stent deformation was distortion, shortening, or severe maldistribution of struts as reported[16].

STATISTICAL ANALYSIS

Only one ISR lesion was analysed per patient. Continuous variables that were non-normally distributed were reported as median with first and third quartiles; normally distributed continuous variables were reported as mean and standard deviation. Comparisons among the groups were performed with the Student's t-test for normally distributed or the Mann-Whitney U test for non-normally distributed continuous variables. Categorical variables were summarised as numbers (percentages) and compared using χ^2 statistics or Fisher's exact test, as appropriate. A multivariable logistic regression model was created to identify factors associated with in-stent neoatherosclerosis; clinically important variables as well as variables statistically significant on univariate analysis were entered into the model. A p-value <0.05 was considered statistically significant. All statistical analyses were performed using SPSS software, Version 22.0 (IBM Corp., Armonk, NY, USA).

Results

CLINICAL CHARACTERISTICS

There were 120 men and 51 women with a mean age of 66.9±11.7 years. Duration from implantation was ≤1 year in 33% of patients (n=57) and >1 year in 66% of patients (n=114). Overall, 122 out of 171 enrolled patients (71.3%) had acute coronary syndrome as the clinical presentation. Among the others, 19 presented with stable angina (11.1%), 27 were without ischaemic symptoms, but had a positive stress test or fractional flow reserve <0.8 (15.8%), and only three (1.8%) had no ischaemia and did not have an intervention. Female sex and adenosine diphosphate antagonist use were more common in the early restenosis group **(Table 1)**. There was no difference in angiographic characteristics between early vs. late DES restenosis other than that left circumflex location was more common in early ISR, and the minimum lumen diameter tended to be larger in the early DES restenosis group **(Table 2)**.

OCT FINDINGS

In OCT-detected second-generation DES restenosis, the MSA was smaller in early vs. late presentation (3.32 mm^2 [interquartile range 2.91-4.41] vs. 3.95 mm^2 [interquartile range 3.28-4.84], p=0.01) **(Figure 2)**, as was the distal reference lumen area **(Table 3)**.

Based on measurements at the MLA site, the ISR pattern was divided into dominant MSA <4.0 mm^2 (MSA <4.0 mm^2 and NIH ≤50%), dominant NIH (MSA ≥4.0 mm^2 and NIH >50%), or mixed (MSA <4.0 mm^2 and NIH >50%). There was a trend for more MSA <4.0 mm^2 in early ISR and more dominant NIH in late ISR **(Figure 3)**.

In-stent neoatherosclerosis was detected in 24.6% of lesions (42/171), with a trend for less neoatherosclerosis in early vs. late ISR (15.5% vs. 28.9%, p=0.06), especially for the presence of calcified NIH (3.5% vs. 20.2%, p=0.004) **(Table 3)**. The distribution of neoatherosclerosis tended to be more focal in early vs. late ISR (89% [8/9] vs. 67% [22/33], p=0.25). Of note, in the current population neoatherosclerosis always clustered within 0.5 mm of the MLA site. There was a significant difference in distribution in the pattern of non-neoatherosclerotic tissue between the two groups: more heterogeneous neointima in early ISR (p=0.049); more homogeneous neointima in late ISR (p=0.04), particularly the high-intensity pattern (p=0.01); and more neointimal thickness <100 μm in early restenosis (p=0.001) **(Figure 4)**. The cumulative prevalence curve also showed that, with time after implantation, there was a less heterogeneous, but a more homogenous pattern with a greater frequency of neoatherosclerosis **(Figure 5)**.

There was no difference in stent fracture, malapposition, or evagination between early vs. late ISR. Overall, the majority of stent fractures/deformation (78.9%), but a minority of malappositions (25.0%) and evaginations (13.0%) occurred at the MLA site **(Table 3)**.

PREDICTORS OF NEOATHEROSCLEROSIS

Multivariable analysis revealed that duration from implantation >2 years (odds ratio [OR]: 2.47, 95% confidence interval [CI]: 1.14-5.35; p=0.02), absence of statin use at the time of ISR (OR: 3.00, 95% CI: 1.22-7.69; p=0.02), and NIH >50% (OR: 3.18, 95%

Table 1. Clinical characteristics.

	Duration from stent implantation		p-value
	≤1 year (n=57)	>1 year (n=114)	
Time since implantation, months	7.7±3.4	40.0±22.9	<0.001
Age, years	66.6±11.7	67.1±11.8	0.78
Female	23 (40.4%)	28 (24.6%)	0.03
Diabetes mellitus	29 (50.9%)	59 (51.8%)	0.91
Hypertension	48 (84.2%)	97 (85.1%)	0.88
Hyperlipidaemia	47 (82.5%)	94 (82.5%)	1.00
Current smoker (<1 month)	9 (15.8%)	13 (11.4%)	0.42
Renal insufficiency*	8 (14.0%)	12 (10.5%)	0.50
Prior myocardial infarction	16 (28.1%)	40 (35.1%)	0.36
Prior coronary artery bypass grafting	16 (28.1%)	20 (17.5%)	0.11
Acute coronary syndromes as clinical presentation	45 (78.9%)	77 (67.5%)	0.12
LDL cholesterol, mg/dL	76.5 (61.0, 100.0)	80.5 (62.0, 107.0)	0.37
HDL cholesterol, mg/dL	41.5 (35.0, 55.0)	41.0 (34.0, 47.0)	0.31
Triglyceride, mg/dL	102.5 (78.0, 147.0)	120.0 (86.0, 165.0)	0.38
Medication at the time of in-stent restenosis			
Statin	47 (82.5%)	96 (84.2%)	0.77
Aspirin	49 (86.0%)	94 (82.5%)	0.56
ADP antagonist	55 (96.5%)	96 (84.2%)	0.02
ACEI/ARB	31 (54.4%)	59 (51.8%)	0.75
Beta-blocker	44 (77.2%)	91 (79.8%)	0.69

Values are n (%) or mean and standard deviation or median (1st quartile, 3rd quartile). *Creatinine clearance <60 mL/min as calculated by the Cockcroft-Gault equation. ACEI: angiotensin-converting enzyme inhibitor; ADP: adenosine diphosphate; ARB: angiotensin receptor blocker; HDL: high-density lipoprotein; LDL: low-density lipoprotein
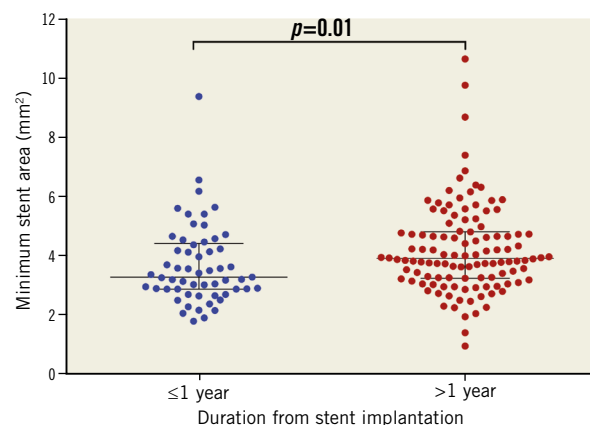

Figure 2. *Minimum stent area among different stents. The minimum stent area was smaller in early compared with late presenting in-stent restenosis (3.32 mm^2 [interquartile range 2.91-4.41] vs. 3.95 mm^2 [interquartile range 3.28-4.84], p=0.01).*

Table 2. Lesion characteristics and quantitative coronary angiography findings.

	Duration from stent implantation		*p*-value
	≤1 year (n=57)	>1 year (n=114)	
Restenotic vessel			
Left anterior descending	25 (43.9%)	61 (53.5%)	0.23
Circumflex	24 (42.1%)	24 (21.1%)	0.004
Right	8 (14.0%)	29 (25.4%)	0.09
Lesion characteristics			
Bifurcation (>1.5 mm)	15 (26.3%)	36 (31.6%)	0.48
Ostial location	7 (12.3%)	15 (13.2%)	0.87
Recurrent restenosis	15 (26.3%)	43 (37.7%)	0.14
In-stent restenosis pattern *			
Type I (focal)	40 (70.2%)	79 (69.3%)	
Type II (diffuse)	8 (14.0%)	25 (21.9%)	0.53
Type III (proliferative)	6 (10.5%)	7 (6.1%)	
Type IV (total occlusion)	3 (5.3%)	2 (1.8%)	
Restenosis lesion length, mm	8.0 (5.6-13.6)	8.3 (5.4-14.3)	0.91
Total old stent length, mm	32.8 (24.2-50.3)	31.6 (17.6-49.9)	0.36
Reference vessel diameter, mm	2.40 (2.09-2.96)	2.60 (2.27-2.89)	0.36
Minimum lumen diameter, mm	1.27 (0.93-1.54)	1.44 (1.09-1.71)	0.07
Diameter stenosis,%	49.6 (36.5-64.0)	44.1 (32.6-56.1)	0.12

Values are n (%) or mean or median with first and third quartiles.
*In-stent restenosis pattern was defined as per Mehran's classification[10].

CI: 1.40-7.21; p=0.01) were independently associated with in-stent neoatherosclerosis **(Table 4)**. If absence of statin use at the time of ISR was replaced with low-density lipoprotein levels, low-density lipoprotein levels were not predictive of neoatherosclerosis.
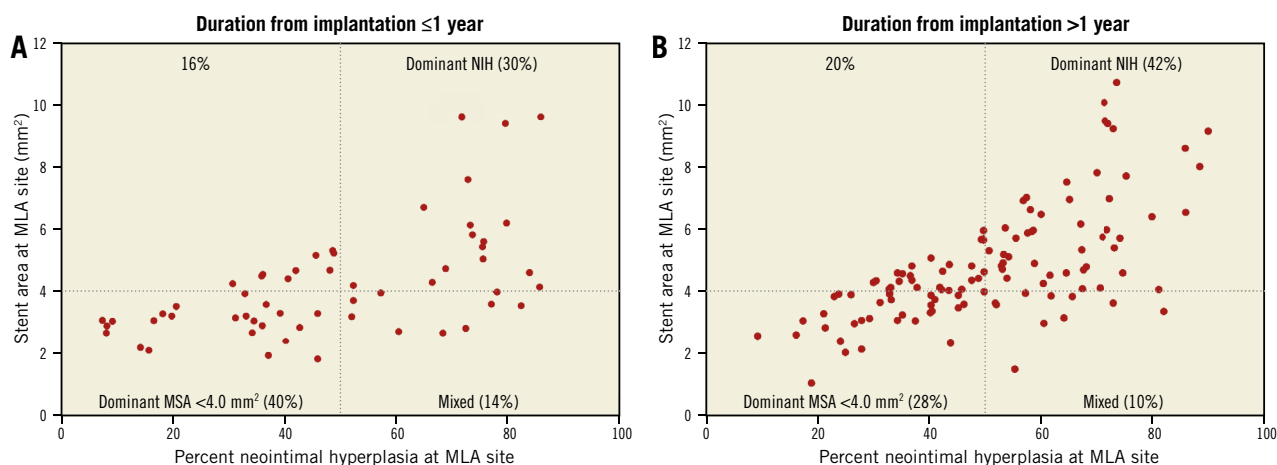
Discussion

The main findings of the current OCT analysis of second-generation DES restenosis were the following. 1) Early second-generation DES restenosis presented more often with an MSA <4.0 mm^2 and heterogeneous hyperplasia. 2) NIH was more frequently observed among late restenoses and included neoatherosclerosis as an important mechanism. 3) Longer duration from stent implantation, absence of statin treatment, and higher NIH burden were independent predictors for neoatherosclerosis.

EARLY ISR

The present study demonstrated that a small stent area was an important factor for early ISR in second-generation DES, especially lesions with an MSA <3.0 mm^2 (35.1% in early vs. 17.5%
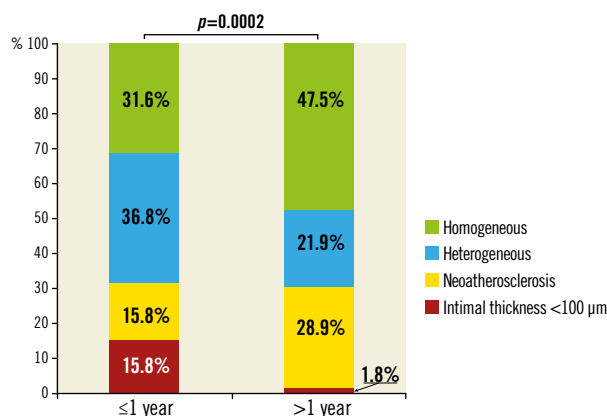

Figure 4. *Pattern of restenotic tissue. Early in-stent restenosis presented more commonly with a non-atherosclerosis pattern of heterogeneous hyperplasia or mean neointimal thickness <100 μm, whereas late in-stent restenosis had more neoatherosclerosis or homogeneous hyperplasia (p=0.0002).*

Figure 3. *Percent neointimal hyperplasia and stent area at minimum lumen area site. Based on the measurements at the minimum lumen area (MLA) site, in-stent restenosis (ISR) was divided into dominant minimum stent area (MSA) <4.0 mm^2 (MSA <4.0 mm^2, neointimal hyperplasia [NIH] ≤50%), dominant NIH (MSA ≥4.0 mm^2 and NIH >50%), and mixed (MSA <4.0 mm^2 and NIH >50%). Early ISR had a trend of more MSA <4.0 mm^2 versus late ISR (40% vs. 28%, p=0.11), whereas late ISR presented with more dominant NIH (42% vs. 30%, p=0.12).*

Table 3. Optical coherence tomography findings.

	Duration from stent implantation		p-value
	≤1 year (n=57)	>1 year (n=114)	
Proximal reference lumen area, mm²	6.83 (5.51-8.10)	6.94 (6.14-8.37)	0.42
Distal reference lumen area, mm²	3.81 (3.02-4.57)	4.74 (3.97-5.68)	0.002
Minimum lumen area, mm²	1.88 (1.37-2.63)	2.19 (1.65-2.58)	0.11
Minimum stent area, mm²	3.32 (2.91-4.41)	3.95 (3.28-4.84)	0.01
Same as minimum lumen area site	30 (52.6%)	63 (55.3%)	0.75
Minimum stent area <4.0 mm²	37 (64.9%)	60 (52.6%)	0.13
Maximal NIH, %	48.8 (33.1-71.7)	51.3 (40.3-67.7)	0.90
Same as MLA site	41 (71.9%)	90 (78.9%)	0.31
Neoatherosclerosis	9 (15.8%)	33 (28.9%)	0.06
Distribution of neoatherosclerosis			0.42
Focal	8 (14.0%)	22 (19.3%)	
Multifocal	0	1 (0.9%)	
Diffuse	1 (1.8%)	10 (8.8)	
Lipidic NIH	8 (14.0%)	17 (14.9%)	0.88
Thin-cap fibroatheroma	3 (5.3%)	7 (6.1%)	1.00
Neointimal rupture	1 (1.8%)	0 (0%)	0.33
Neointimal calcium	2 (3.5%)	23 (20.2%)	0.004
Neointimal macrophages	18 (31.6%)	56 (49.1%)	0.03
Maximal angle, °	148 (115-246)	147 (99-199)	0.28
Microvessels	7 (12.3%)	38 (33.3%)	0.01
Peri-strut low-intensity area	38 (66.7%)	58 (50.9%)	0.05
Thrombus	2 (3.5%)	12 (10.5%)	0.15
Stent fracture/deformation	6 (10.5%)	13 (11.4%)	0.86
Located at MLA site	5 (8.8%)	10 (8.8%)	1.00
Stent fracture	4 (7.0%)	8 (7.0%)	1.00
Stent deformation	2 (3.5%)	7 (6.1%)	0.72
Malapposition	17 (29.8%)	23 (20.2%)	0.16
Located at MLA site	6 (10.5%)	4 (3.5%)	0.09
Evagination	9 (15.8%)	14 (12.3%)	0.53
Located at MLA site	2 (3.5%)	1 (0.9%)	0.26

Values are n (%) or median with first and third quartiles. MLA: minimum lumen area; NIH: neointimal hyperplasia
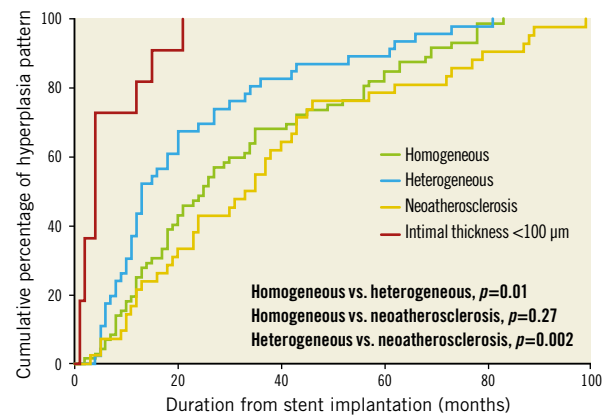

Figure 5. *Cumulative percentage of restenotic pattern with duration from implantation. Over time there was less heterogeneous neointimal hyperplasia (NIH) or mean neointimal thickness <100 μm, but more homogenous NIH and neoatherosclerosis was found with greater frequency.*

A serial IVUS study by Sonoda et al[18] suggested that the cut-off values of the post-procedure MSA to predict freedom from restenosis at eight months were 6.5 mm² for BMS and 5.0 mm² for sirolimus-eluting stents. A similar study by Song et al[20] demonstrated the thresholds of 5.5 mm² for sirolimus-eluting stents, 5.3 mm² for zotarolimus-eluting stents, and 5.4 mm² for EES. A small stent area reflected both stent underexpansion and/or implantation into a small vessel, as shown by the fact that there was no significant difference for the MSA/distal reference lumen area ratio between early vs. late ISR[22]. In the recent IVUS-XPL study, Hong et al[19] demonstrated that an IVUS-optimised MSA (MSA greater than the distal reference lumen CSA) was protective for one-year MACE after EES implantation (1.5% vs. 4.6%, p=0.02).

In the current study, a heterogeneous pattern of neointima was observed in early ISR. This was believed to represent a process of healing where glycosaminoglycan proteins were substituted for smooth muscle cells and collagen matrix (**Figure 4**, **Figure 5**)[23]. Chung et al[24] showed that a speckled neointimal pattern (similar to the heterogeneous, non-layered pattern in our current study) represented myxomatous tissue containing extracellular matrix enriched with proteoglycans that decreased over time to be replaced by matured smooth muscle cells or collagen deposition; a layered pattern, similar to peri-strut low-intensity area, was considered to represent the presence of fibrinoid or proteoglycans, another reflection of delayed arterial healing[6,14]. This process was usually completed within 28 days for BMS[25], but was delayed after DES implantation[26]. Because of its retrospective design, the current study could not deduce a sequenced relationship between these two image patterns. Notably, an angioscopy study from Sera et al[21] showed that inadequate stent expansion was associated with angioscopically incomplete neointimal coverage after sirolimus-eluting stent implantation.

in late ISR, p=0.01). A larger stent area provided more room to accommodate NIH (bigger-is-better paradigm). Castagna et al[17] reported that 20% of 1,090 BMS restenosis lesions had an intravascular ultrasound (IVUS) MSA <5.0 mm². In the DES era, the prevalence of underexpansion as a cause of ISR has increased compared with BMS, although the threshold was reduced when NIH was inhibited[18]; more than 50% of cases in the current study had an OCT MSA <4 mm², consistent with other DES studies[19-21].

Table 4. Predictors of in-stent neoatherosclerosis.

	Neoatheroscle-rosis (n=42)	Non-neoathero-sclerosis (n=129)	Univariable		Multivariable	
			Odds ratio (95% CI)	*p*-value	Odds ratio (95% CI)	*p*-value
Age >65 years	22 (52.4%)	73 (56.6%)	1.19 (0.58-2.42)	0.64		
Duration from implantation >2 years	24 (57.1%)	51 (39.5%)	2.04 (1.01-4.13)	0.048	2.47 (1.14-5.35)	0.02
Female	14 (33.3%)	37 (28.7%)	1.24 (0.59-2.62)	0.57		
Diabetes	21 (50.0%)	67 (51.9%)	0.93 (0.46-1.86)	0.83		
Renal insufficiency	5 (11.9%)	15 (11.6%)	1.03 (0.35-3.02)	0.96		
Current smoker	4 (9.5%)	18 (14.0%)	0.65 (0.21-2.04)	0.46		
ACEI/ARB at the time of ISR	22 (52.4%)	68 (52.7%)	0.99 (0.49-1.98)	0.97		
Absence of statin use at the time of ISR	30 (71.4%)	113 (87.6%)	2.86 (1.20-6.67)	0.02	3.00 (1.22-7.69)	0.02
Prior ISR history	17 (40.5%)	41 (31.8%)	1.46 (0.71-3.00)	0.30		
MSA <4.0 mm^2	18 (42.9%)	79 (61.2%)	0.48 (0.23-0.96)	0.04		
NIH >50%	30 (71.4%)	58 (45.0%)	3.06 (1.44-6.51)	0.004	3.18 (1.40-7.21)	0.01

Values are n (%), mean and standard deviation, or median with first and third quartiles. Variables entered into the multivariable model: duration from implantation >2 years, statins at the time of ISR, MSA <4.0 mm^2, NIH >50%. ACEI: angiotensin-converting enzyme inhibitor; ARB: angiotensin receptor blocker; ISR: in-stent restenosis; MSA: minimum stent area; NIH: neointimal hyperplasia

LATE RESTENOSIS

In-stent neoatherosclerosis has been associated with late DES failure in an OCT study by Kang et al[7]. Our findings are consistent with this and supported by a pathology study in second-generation DES (48% prevalence in late vs. 17% in early ISR)[27]. Unlike in BMS where neoatherosclerosis occurred almost exclusively after three years, neoatherosclerosis in second-generation DES appeared early and increased over time. Calcified NIH was observed more often in late ISR, also consistent with a previous autopsy study[13,27], and similar to progression of atherosclerotic plaques in native arteries[28]. Our findings of microvessels and macrophages in late neointima indicated their role in atherosclerotic progression and late restenosis, consistent with OCT literature[6,7]. Histopathological studies have shown that microvessels usually expand from adventitia into plaque, and circulating macrophages infiltrate through the vasa vasorum. The infiltration of activated macrophages and deposition of foam cells might have induced the development of neoatherosclerosis and plaque destabilisation[27,29].

Predictors for neoatherosclerosis in second-generation DES have been less well established. In previous studies, longer implant duration (≥48 months), first-generation DES (versus BMS), current smoking, chronic kidney disease, absence of angiotensin-converting enzyme inhibitors or angiotensin II receptor blockers, and underlying unstable plaques were independent predictors for neoatherosclerosis[13,29]. A more recent study including second-generation DES reported that chronic kidney disease, low-density lipoprotein cholesterol >70 mg/dL, and stent age were predictors for neoatherosclerosis, whereas the type of DES was not a predictor[30]. In the present study, we found that neoatherosclerosis occurred less frequently in lesions with an MSA <4.0 mm^2 (32.4% vs. 18.6%, p=0.04) due to the absence of NIH, the foundation for neoatherosclerosis development. Acute coronary syndromes accounted for over 70% of clinical presentations, especially in late ISR and in lesions with lipidic NIH, emphasising the importance of risk factor control even after stent implantation.

Study limitations

This is a retrospective study, and most patients presented with symptoms or ischaemia. Second, the present study is not a serial analysis. Third, the definition of ISR was based on OCT instead of angiographic diameter stenosis (49.6% [36.5-64.0] in the early and 44.1% [32.6-56.1] in the late group), which may not be an adequate definition; however, all but three patients had demonstrable ischaemia. Fourth, as recently reported by Lutter et al, OCT has intrinsic limitations in the qualitative analysis of restenotic tissue; histopathologic equivalency should be interpreted with caution[31]. However, even in their study, the diagnostic accuracy of OCT was greater in restenotic lesions. Nevertheless, the definition of OCT-neoatherosclerosis has varied among studies in the literature and needs further clarification or validation or the use of combined imaging devices to include near-infrared spectroscopy or other technique of tissue characterisation[32]. Fifth, the cut-off for defining significant luminal narrowing and underexpansion is still a matter of debate. Sixth, reference lumen area assessment was limited by the length of pullback and was available in only 77% (131/171). Seventh, the reasons why patients were not treated with statins were not collected. Finally, because of the sample size, we could not demonstrate distinctive properties among different types of second-generation DES.

Conclusions

The OCT morphological characteristics of second-generation DES restenotic tissue were different between early vs. late presentation. Early restenosis was associated with MSA <4.0 mm^2 while neoatherosclerosis contributed to late ISR.

Impact on daily practice

When in-stent restenosis is found in a second-generation DES <1 year after implantation, nearly half of the cases may have stent underexpansion. When in-stent restenosis is found in a second-generation DES after one year, about 1/3 of the cases may have neoatherosclerosis including neointimal calcification. OCT should be considered before decision making when treating in-stent restenosis to clarify the underlying causes.

Conflict of interest statement

L. Song has received a research grant from Boston Scientific. G. Mintz is a consultant for Boston Scientific and ACIST, has received fellowship/grant support from Volcano, Boston Scientific, and Infraredx, and honoraria from Boston Scientific and ACIST. C.Y. Chin has received honoraria from ACIST. A. Kirtane has received institutional research grants to Columbia University from Boston Scientific, Medtronic, Abbott Vascular, Abiomed, St. Jude Medical, and Eli Lilly. M. Parikh is on the speakers bureau for Abbott Vascular, Boston Scientific, Medtronic, CSI, Corindus, and is on the advisory board of Abbott Vascular, Medtronic, and Philips. J. Moses is a consultant for Abiomed. Z. Ali has received grant support from and is a consultant for St. Jude Medical. R. Shlofmitz is a speaker for CSI. A. Maehara has received grant support from Boston Scientific and St. Jude Medical for research fellows, is a consultant for Boston Scientific and OCT Medical Imaging, and has received speaker fees from St. Jude Medical. The other authors have no conflicts of interest to declare.

References

1. Stone GW, Rizvi A, Sudhir K, Newman W, Applegate RJ, Cannon LA, Maddux JT, Cutlip DE, Simonton CA, Sood P, Kereiakes DJ; SPIRIT IV Investigators. Randomized comparison of everolimus- and paclitaxel-eluting stents. 2-year follow-up from the SPIRIT (Clinical Evaluation of the XIENCE V Everolimus Eluting Coronary Stent System) IV trial. *J Am Coll Cardiol.* 2011;58:19-25.

2. Silber S, Windecker S, Vranckx P, Serruys PW; RESOLUTE All Comers investigators. Unrestricted randomised use of two new generation drug-eluting coronary stents: 2-year patient-related versus stent-related outcomes from the RESOLUTE All Comers trial. *Lancet.* 2011;377:1241-7.

3. Gada H, Kirtane AJ, Newman W, Sanz M, Hermiller JB, Mahaffey KW, Cutlip DE, Sudhir K, Hou L, Koo K, Stone GW. 5-year results of a randomized comparison of XIENCE V everolimus-eluting and TAXUS paclitaxel-eluting stents: final results from the SPIRIT III trial (clinical evaluation of the XIENCE V everolimus eluting coronary stent system in the treatment of patients with de novo native coronary artery lesions). *JACC Cardiovasc Interv.* 2013;6:1263-6.

4. Valgimigli M, Tebaldi M, Borghesi M, Vranckx P, Campo G, Tumscitz C, Cangiano E, Minarelli M, Scalone A, Cavazza C, Marchesini J, Parrinello G; PRODIGY Investigators. Two-year outcomes after first- or second-generation drug-eluting or bare-metal stent implantation in all-comer patients undergoing percutaneous coronary intervention: a pre-specified analysis from the PRODIGY study (PROlonging Dual Antiplatelet Treatment After Grading stent-induced Intimal hyperplasia studY). *JACC Cardiovasc Interv.* 2014;7:20-8.

5. Sen H, Lam MK, Lowik MM, Danse PW, Jessurun GA, van Houwelingen KG, Anthonio RL, Tjon Joe Gin RM, Hautvast RW, Louwerenburg JH, de Man FH, Stoel MG, van der Heijden LC, Linssen GC, IJzerman MJ, Tandjung K, Doggen CJ, von Birgelen C. Clinical Events and Patient-Reported Chest Pain in All-Comers Treated With Resolute Integrity and Promus Element Stents: 2-Year Follow-Up of the DUTCH PEERS (DUrable Polymer-Based STent CHallenge of Promus ElemEnt Versus ReSolute Integrity) Randomized Trial (TWENTE II). *JACC Cardiovasc Interv.* 2015;8:889-99.

6. Habara M, Terashima M, Nasu K, Kaneda H, Yokota D, Ito T, Kurita T, Teramoto T, Kimura M, Kinoshita Y, Tsuchikane E, Asakura Y, Suzuki T. Morphological differences of tissue characteristics between early, late, and very late restenosis lesions after first generation drug-eluting stent implantation: an optical coherence tomography study. *Eur Heart J Cardiovasc Imaging.* 2013;14:276-84.

7. Kang SJ, Mintz GS, Akasaka T, Park DW, Lee JY, Kim WJ, Lee SW, Kim YH, Whan Lee C, Park SW, Park SJ. Optical coherence tomographic analysis of in-stent neoatherosclerosis after drug-eluting stent implantation. *Circulation.* 2011;123:2954-63.

8. Bezerra HG, Attizzani GF, Sirbu V, Musumeci G, Lortkipanidze N, Fujino Y, Wang W, Nakamura S, Erglis A, Guagliumi G, Costa MA. Optical coherence tomography versus intravascular ultrasound to evaluate coronary artery disease and percutaneous coronary intervention. *JACC Cardiovasc Interv.* 2013;6:228-36.

9. Goto K, Zhao Z, Matsumura M, Dohi T, Kobayashi N, Kirtane AJ, Rabbani LE, Collins MB, Parikh MA, Kodali SK, Leon MB, Moses JW, Mintz GS, Maehara A. Mechanisms and Patterns of Intravascular Ultrasound In-Stent Restenosis Among Bare Metal Stents and First- and Second-Generation Drug-Eluting Stents. *Am J Cardiol.* 2015;116:1351-7.

10. Mehran R, Dangas G, Abizaid AS, Mintz GS, Lansky AJ, Satler LF, Pichard AD, Kent KM, Stone GW, Leon MB. Angiographic patterns of in-stent restenosis: classification and implications for long-term outcome. *Circulation.* 1999;100:1872-8.

11. Gonzalo N, Serruys PW, Okamura T, van Beusekom HM, Garcia-Garcia HM, van Soest G, van der Giessen W, Regar E. Optical coherence tomography patterns of stent restenosis. *Am Heart J.* 2009;158:284-93.

12. Prati F, Guagliumi G, Mintz GS, Costa M, Regar E, Akasaka T, Barlis P, Tearney GJ, Jang IK, Arbustini E, Bezerra HG, Ozaki Y, Bruining N, Dudek D, Radu M, Erglis A, Motreff P, Alfonso F, Toutouzas K, Gonzalo N, Tamburino C, Adriaenssens T, Pinto F, Serruys PW, Di Mario C; Expert's OCT Review Document. Expert review document part 2: methodology, terminology and clinical applications of optical coherence tomography for the assessment of interventional procedures. *Eur Heart J.* 2012;33:2513-20.

13. Nakazawa G, Otsuka F, Nakano M, Vorpahl M, Yazdani SK, Ladich E, Kolodgie FD, Finn AV, Virmani R. The pathology of neoatherosclerosis in human coronary implants bare-metal and drugeluting stents. *J Am Coll Cardiol.* 2011;57:1314-22.

14. Teramoto T, Ikeno F, Otake H, Lyons JK, van Beusekom HM, Fearon WF, Yeung AC. Intriguing peri-strut low-intensity area detected by optical coherence tomography after coronary stent deployment. *Circ J.* 2010;74:1257-9.

15. Radu MD, Raber L, Kalesan B, Muramatsu T, Kelbaek H, Heo J, Jorgensen E, Helqvist S, Farooq V, Brugaletta S, Garcia-Garcia HM, Jüni P, Saunamäki K, Windecker S, Serruys PW. Coronary evaginations are associated with positive vessel remodelling and are nearly absent following implantation of newer-generation drug-eluting stents: an optical coherence tomography and intravascular ultrasound study. *Eur Heart J.* 2014;35:795-807.

16. Inaba S, Mintz GS, Yun KH, Yakushiji T, Shimizu T, Kang SJ, Généreux P, Weisz G, Rabbani LE, Moses JW, Stone GW, Maehara A. Mechanical complications of everolimus-eluting stents associated with adverse events: an intravascular ultrasound study. *EuroIntervention.* 2014;9:1301-8.

17. Castagna MT, Mintz GS, Leiboff BO, Ahmed JM, Mehran R, Satler LF, Kent KM, Pichard AD, Weissman NJ. The contribution of "mechanical" problems to in-stent restenosis: An intravascular ultrasonographic analysis of 1090 consecutive in-stent restenosis lesions. *Am Heart J.* 2001;142:970-4.

18. Sonoda S, Morino Y, Ako J, Terashima M, Hassan AH, Bonneau HN, Leon MB, Moses JW, Yock PG, Honda Y, Kuntz RE, Fitzgerald PJ; SIRIUS Investigators. Impact of final stent dimensions on long-term results following sirolimus-eluting stent implantation: serial intravascular ultrasound analysis from the sirius trial. *J Am Coll Cardiol.* 2004;43:1959-63.

19. Hong SJ, Kim BK, Shin DH, Nam CM, Kim JS, Ko YG, Choi D, Kang TS, Kang WC, Her AY, Kim YH, Hur SH, Hong BK, Kwon H, Jang Y, Hong MK; IVUS-XPL Investigators. Effect of Intravascular Ultrasound-Guided vs Angiography-Guided Everolimus-Eluting Stent Implantation: The IVUS-XPL Randomized Clinical Trial. *JAMA.* 2015;314:2155-63.

20. Song HG, Kang SJ, Ahn JM, Kim WJ, Lee JY, Park DW, Lee SW, Kim YH, Lee CW, Park SW, Park SJ. Intravascular ultrasound assessment of optimal stent area to prevent in-stent restenosis after zotarolimus-, everolimus-, and sirolimus-eluting stent implantation. *Catheter Cardiovasc Interv.* 2014;83:873-8.

21. Sera F, Awata M, Uematsu M, Kotani J, Nanto S, Nagata S. Optimal stent-sizing with intravascular ultrasound contributes to complete neointimal coverage after sirolimus-eluting stent implantation assessed by angioscopy. *JACC Cardiovasc Interv.* 2009;2:989-94.

22. Bertrand OF, De Larochelliere R, Joyal M, Bonan R, Mongrain R, Tardif JC. Incidence of stent under-deployment as a cause of in-stent restenosis in long stents. *Int J Cardiovasc Imaging.* 2004;20:279-84.

23. Nakano M, Vorpahl M, Otsuka F, Taniwaki M, Yazdani SK, Finn AV, Ladich ER, Kolodgie FD, Virmani R. Ex vivo assessment of vascular response to coronary stents by optical frequency domain imaging. *JACC Cardiovasc Imaging.* 2012;5:71-82.

24. Chung IM, Gold HK, Schwartz SM, Ikari Y, Reidy MA, Wight TN. Enhanced extracellular matrix accumulation in restenosis of coronary arteries after stent deployment. *J Am Coll Cardiol.* 2002;40:2072-81.

25. Farb A, Sangiorgi G, Carter AJ, Walley VM, Edwards WD, Schwartz RS, Virmani R. Pathology of acute and chronic coronary stenting in humans. *Circulation.* 1999;99:44-52.

26. Joner M, Finn AV, Farb A, Mont EK, Kolodgie FD, Ladich E, Kutys R, Skorija K, Gold HK, Virmani R. Pathology of drug-eluting stents in humans: delayed healing and late thrombotic risk. *J Am Coll Cardiol.* 2006;48:193-202.

27. Otsuka F, Vorpahl M, Nakano M, Foerst J, Newell JB, Sakakura K, Kutys R, Ladich E, Finn AV, Kolodgie FD, Virmani R. Pathology of second-generation everolimus-eluting stents versus first-generation sirolimus- and paclitaxel-eluting stents in humans. *Circulation.* 2014;129:211-23.

28. Mintz GS, Pichard AD, Popma JJ, Kent KM, Satler LF, Bucher TA, Leon MB. Determinants and correlates of target lesion calcium in coronary artery disease: a clinical, angiographic and intravascular ultrasound study. *J Am Coll Cardiol.* 1997;29: 268-74.

29. Yonetsu T, Kato K, Kim SJ, Xing L, Jia H, McNulty I, Lee H, Zhang S, Uemura S, Jang Y, Kang SJ, Park SJ, Lee S, Yu B, Kakuta T, Jang IK. Predictors for neoatherosclerosis: a retrospective observational study from the optical coherence tomography registry. *Circ Cardiovasc Imaging.* 2012;5:660-6.

30. Lee SY, Hur SH, Lee SG, Kim SW, Shin DH, Kim JS, Kim BK, Ko YG, Choi D, Jang Y, Hong MK. Optical coherence tomographic observation of in-stent neoatherosclerosis in lesions with more than 50% neointimal area stenosis after second-generation drug-eluting stent implantation. *Circ Cardiovasc Interv.* 2015;8:e001878.

31. Lutter C, Mori H, Yahagi K, Ladich E, Joner M, Kutys R, Fowler D, Romero M, Narula J, Virmani R, Finn AV. Histopathological Differential Diagnosis of Optical Coherence Tomographic Image Interpretation After Stenting. *JACC Cardiovasc Interv.* 2016;9:2511-2523.

32. Ali ZA, Roleder T, Narula J, Mohanty BD, Baber U, Kovacic JC, Mintz GS, Otsuka F, Pan S, Virmani R, Sharma SK, Moreno P, Kini AS. Increased thin-cap neoatheroma and periprocedural myocardial infarction in drug-eluting stent restenosis: multimodality intravascular imaging of drug-eluting and bare-metal stents. *Circ Cardiovasc Interv.* 2013;6:507-17.